

## Thermal evolution of the Gangdese batholith, southern Tibet: A history of episodic unroofing

Peter Copeland,<sup>1</sup> T. Mark Harrison,<sup>2</sup> Pan Yun,<sup>3</sup> W.S.F. Kidd,<sup>3</sup> Mary Roden,<sup>4</sup> and Zhang Yuquan<sup>5</sup>

**Abstract.** The Gangdese batholith, southern Tibet, was part of an Andean-type arc at the southern margin of Asia prior to the collision of India and Asia at approximately 50 to 40 Ma. Fission-track and  $^{40}\text{Ar}/^{39}\text{Ar}$  analyses of 28 rocks from 10 Gangdese granitoid plutons along an ~250 km length of the batholith in the Lhasa region provide a detailed understanding of the age and the postcrystallization erosional and tectonic history of these rocks. These data suggest a range of ages for these plutons of 94 to 42 Ma, with the majority being of Tertiary age. The postcrystallization cooling histories of all of these plutons are characterized by marked discontinuities. We conclude that most of these discontinuities, and all of them after 40 Ma, reflect tectonic changes that produced brief pulses of rapid erosion which were distributed in both space and time. In addition to the initial cooling of hot magma against cold country rock, all of the rocks we studied showed evidence for at least one subsequent episode of rapid cooling, dropping many tens of degrees in a few million years. Conversely, these plutons all experienced intervals during which they cooled very slowly or not at all; these slow-cooling intervals lasted from 5 to 50 million years. Our data indicate that since the collision between India and Asia began, response to continued convergence has been quite variable in even this relatively small area. The data reported here are consistent with a recently-proposed model of Oligo-Miocene crustal shortening along the Gangdese Thrust system in this area.

### Introduction

Our understanding of how the lithosphere responds to continental collision was revolutionized in the light of plate tectonic theory [e.g., *Dewey and Bird*, 1970]. Although the subsequent decades brought a vastly improved understanding of the details of orogeny, this was accompanied by recognition that the behavior of the continental lithosphere under tectonic forces is of far greater complexity than that of the oceanic crust [e.g., *Molnar and Tapponnier*, 1975]. The multiplicity

of modes by which continents respond to plate motions places a premium on knowing the timing and duration of each deformation mechanism. The contributions of radiogenic isotope investigations to the understanding of the evolution of mountain belts are both direct, such as determining the timing of fault motion, and inferential, such as deducing the timing of crustal thickening from denudation rates. The Tertiary Indo-Asian orogeny presents a unique opportunity to use both direct and inferential evidence to examine active and ancient manifestations of the collision of two continental masses.

Before the start of the collision between India and Asia at about 50 Ma the southern margin of Asia was marked by an Andean-type arc, known as the Gangdese or Transhimalayan batholith. The batholith marking the roots of this arc, which lies 100 to 200 km north of the Himalaya and stretches E-W for over 2000 km across southern Tibet and northern India, varies between 20 and 60 km wide (Figure 1). In many places the suture marking the closure of the Tethyan ocean lies immediately to the south of the batholith. The plutonic rocks of the Gangdese batholith have a range of crystallization ages from ~120 Ma to 40 Ma [*Harris et al.*, 1988b; *Schärer and Allègre*, 1984] and a wide variation in composition including gabbro, granite, and tonalite; the average composition is granodiorite [*Debon et al.*, 1986]. The youngest Gangdese plutons are approximately 40 Ma [*Schärer and Allègre*, 1984], suggesting that subduction of the ocean crust that once separated India from Asia may be continued to about that time.

This paper presents  $^{40}\text{Ar}/^{39}\text{Ar}$  and fission-track data from ten plutons of the eastern Gangdese batholith related to both the timing of thrust faulting affecting the batholith and its denudation consequent upon the crustal thickening episode. This study focuses on an ~225-km-long segment of the Gangdese batholith in the Lhasa region (Figure 2) and provides documentation on what happens to large volcanic-plutonic arcs when modified by continental collision.

### Analytical Procedures

Thirty-six minerals from 16 samples of 10 Gangdese plutons at nine locations were analyzed by the  $^{40}\text{Ar}/^{39}\text{Ar}$  method; one mineral from a sample of country rock was also studied. The analytical procedures followed those discussed by Copeland [1990] and Harrison and FitzGerald [1986]. With the exception of sample XR-2a, tabulated results of the  $^{40}\text{Ar}/^{39}\text{Ar}$  analysis are given by Copeland [1990] and all are available from the first author upon request.

In this study we assume that the argon diffusion behavior of hornblende and biotite are reasonably-well described by the results of diffusion studies utilizing hydrothermal conditions (see, for example, *Harrison* [1981], *Harrison et al.* [1985], and *Copeland et al.* [1987]). To wit, for hornblende  $E \cong 60,000$  cal/mol,  $D_0 \cong 0.024$  cm<sup>2</sup>/s,  $a \cong 0.004$  cm; and for biotite  $E \cong 47,000$  cal/mole,  $D_0 \cong 0.077$  cm<sup>2</sup>/s,  $a \cong 0.031$  cm.

<sup>1</sup>Department of Geosciences, University of Houston, Houston, Texas.

<sup>2</sup>Department of Earth and Space Sciences and Institute of Geophysics and Space Physics, University of California, Los Angeles.

<sup>3</sup>Department of Geological Sciences, State University of New York at Albany.

<sup>4</sup>Department of Geology, Rensselaer Polytechnic Institute, Troy, New York.

<sup>5</sup>Institute of Geochemistry, Academia Sinica, Guyang, People's Republic of China.

Copyright 1995 by the American Geophysical Union.

Paper number 94TC01676.

0278-7407/95/94TC-01676\$10.00

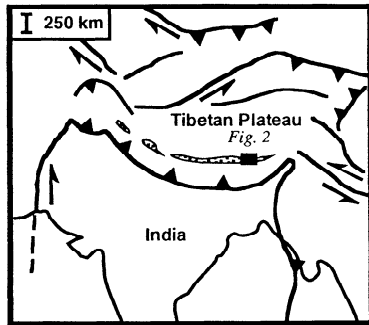


**Figure 1.** Generalized tectonic map of Asia showing major crustal-scale faults. The approximate location of the Gangdese batholith is shown by the stippled pattern; the area of Figure 2 is shown by the solid rectangle.

K-feldspars analyzed in this study appear to contain a discrete distribution of diffusion domain sizes that varies widely between samples, precluding our use of a single set of characteristic diffusion parameters. However, the general stability

of K-feldspars during laboratory heating [FitzGerald and Harrison, 1993; Lovera et al., 1993] permits us to acquire Arrhenius parameters specific to each sample [Harrison and McDougall, 1981; Lovera et al., 1989]. All of the K-feldspars in this study exhibit Arrhenius relationships which are characteristic of samples containing multiple diffusion domains [Lovera et al., 1989, 1991, 1993]. A sample containing only one diffusion domain would plot as a line on an Arrhenius diagram with a slope proportional to the activation energy of the diffusion domain and y-axis intercept equal to the diffusion coefficient at infinite temperature divided by the square of the diffusion lengthscale ( $D_0/r^2$ ). All of the samples in the present study show an initial linear segment on the Arrhenius diagram, followed by a deviation to a curvilinear segment representing larger diffusion domains.

The multi-diffusion-domain approach uses forward modeling of the Arrhenius plot to find the distribution of relative sizes and volume fractions of diffusion domains in the sample. Once both the distribution and Arrhenius parameters are acquired, a thermal history can be calculated by iteratively fitting model age spectra to the empirical results. This approach

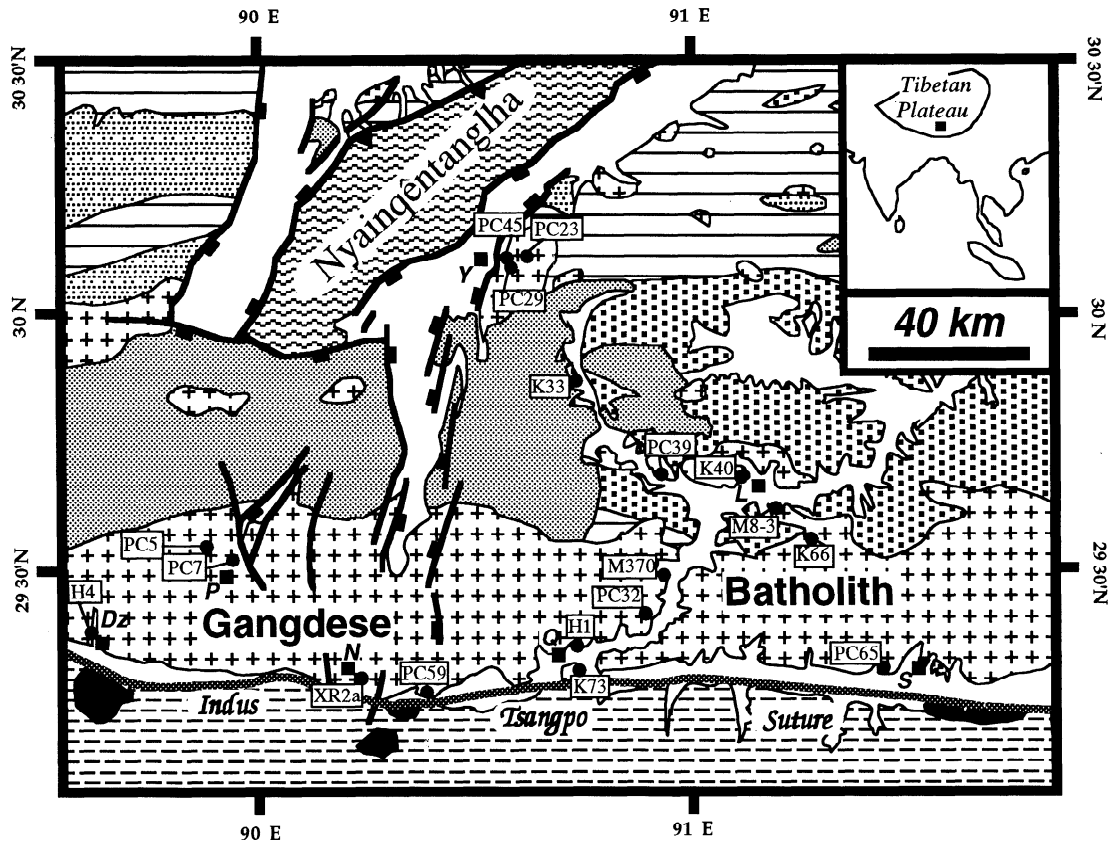


**Figure 2.** Simplified geologic map of the study area, southern Tibet [after Kidd et al., 1988]. Crosses are granitoid rocks (and undifferentiated enclaves of metamorphic and sedimentary rocks) of the Gangdese batholith; gray shaded areas, Tertiary ignimbrites (Linziqong Formation); dots, Mesozoic sedimentary and volcanic rocks; horizontal lines, Paleozoic sedimentary rocks; solid areas, ophiolites; dashed lines, "Tethyan" Mesozoic sedimentary rocks of the Indian plate. Thick solid lines are faults; north-south faults are Miocene to Recent normal faults. Sample sites shown with abbreviated name (e.g., PC45, PC-88-45). Some sample sites account for more than one sample as follows: PC7 is PC7, PC11, and PC12, PC30, PC30 and PC32; PC39, PC39 and PC36; K40, K40, K42, and K45; K66, K66 and K72; H1, H1 and H2; M370, M369, M370, M371, M372, and M373. Squares indicate towns and villages: Y is Yangbajian, L, Lhasa, D, Dagze, S, Samye, Q, Quxu, P, Pachu, Dz, Dazhuka. N, Nyemo.

**Table 1.** Apatite Fission Track Data

Sample	Pluton	Number of Grains	density of tracks ( $10^6 / \text{cm}^2$ )		Model [U], ppm	$\chi^2, \%$	Lithology	Age $\pm 1\sigma$ , Ma	Elevation, m
			$\rho_d$	$\rho_s$					
M369	Quxu	17	4.261	0.377	4.72	20	granodiorite	(16.4 $\pm$ 1.5)	4600
M370	Quxu	20	4.221	0.432	4.88	80	granodiorite	16.2 $\pm$ 1.2	4350
M371	Quxu	10	4.181	0.627	7.46	95	granodiorite	15.9 $\pm$ 1.3	4100
M372	Quxu	10	4.141	0.368	4.51	90	granodiorite	15.3 $\pm$ 1.4	3850
M373	Quxu	25	4.191	0.929	11.8	80	granodiorite	15.0 $\pm$ 0.9	3600
H-88-1	Quxu	16	4.021	0.456	4.47	10	granodiorite	18.6 $\pm$ 1.5	3800
H-88-2	Quxu	10	4.583	0.564	5.48	1	granodiorite	(21.4 $\pm$ 2.9)	3600
K-88-3	Quxu	20	4.459	0.0854	1.13	30	dacite	15.2 $\pm$ 2.5	4400
K-88-33(A)	Machu	14	3.881	0.161	0.626	98	diorite	45.2 $\pm$ 5.9	3870
K-88-33(B)	Machu	12	3.919	0.207	0.781	70	diotite	47.0 $\pm$ 5.5	3870
K-88-45	Lhasa	8	3.764	0.255	1.72	30	granite	25.2 $\pm$ 4.3	3720
K-88-66	Dagze	10	4.113	0.250	1.40	50	granite	33.3 $\pm$ 5.2	5050
K-88-72	Dagze	20	3.981	0.347	3.27	80	granite	19.1 $\pm$ 2.1	3975
K-88-73	Quxu	12	4.152	0.494	4.59	70	granodiorite	20.2 $\pm$ 1.6	3440
PC-88-11	Pachu	22	4.365	0.214	2.78	80	granodiorite	15.1 $\pm$ 2.1	4600
PC-88-12	Pachu	15	4.301	0.186	2.12	99	granodiorite	17.1 $\pm$ 2.2	4200
PC-88-29	Yangbajian	20	4.341	0.739	15.3	90	granite	9.5 $\pm$ 0.9	4300
PC-88-30	Quxu	20	4.253	0.544	5.41	70	granite	19.4 $\pm$ 1.5	3760
PC-88-32	Quxu	20	4.211	0.165	1.74	98	granite	18.1 $\pm$ 1.7	4560
PC-88-36	Gu Rong	20	4.061	0.581	5.12	50	granite	20.8 $\pm$ 1.7	4500
PC-88-39(A)	Gu Rong	21	3.941	0.394	3.54	30	granite	19.9 $\pm$ 1.8	3750
PC-88-39(B)	Gu Rong	12	4.005	0.690	6.23	70	granite	20.1 $\pm$ 1.7	3750
PC-88-59	Neymo	30	4.230	0.208	5.76	50	granite	6.9 $\pm$ 0.9	3700
PC-88-62	Samye	22	4.280	0.301	2.09	50	tonalite	27.5 $\pm$ 3.3	4440
PC-88-65	Samye	20	4.348	0.331	2.61	80	tonalite	24.9 $\pm$ 2.3	3750

External detector method used for these analyses. Abbreviations are  $\rho_d$ , density;  $\rho_s$ , spontaneous track density;  $\rho_i$ , induced track density. The  $\chi^2$  statistics (the probability of obtaining  $\chi^2 = \text{value}$  for  $n$  degrees of freedom where  $n$  equals the number of crystals minus 1) were used to assess the scattering of individual grain dates. Ages in parentheses were calculated using the mean ( $\rho_s/\rho_i$ ). A and B after sample name indicate two analyses of the same sample from two packages

is discussed in detail elsewhere [e.g., *Lovera et al.*, 1989; *Richter et al.*, 1991]. Most of the  $^{40}\text{Ar}/^{39}\text{Ar}$  results reported in this study were acquired at a time when optimum experimental conditions for K-feldspars were not yet established (for a discussion of these procedures see *Lovera et al.* [1993]) and thus these results provide somewhat more limited thermal history information than what might be expected from current procedures. Nonetheless, significant constraints can yet be obtained from these samples. It is for this reason that we emphasize this multidomain approach only for selected samples where detailed thermal histories are pivotal in establishing changes in denudation rates.

It has been shown that modeling following this approach is insensitive to the number of diffusion domains, as long as an appropriate minimum number is used. In other words, in a given case, the actual number may be four; in such a situation, as long as the number of model domains is greater than three, the cooling history derived from the modeling will not be significantly altered. Any approach not acknowledging a domain structure (of whatever distribution) is implicitly modeling feldspars as a single, uniform diffusion domain; this approach clearly does not yield thermal histories similar to those obtained from other independent methods [see for example, *Richter et al.*, 1991]. The thermal histories obtained from this modeling are also insensitive to the diffusion geometry chosen (*i.e.*, slab or sphere) and the form of the cooling history.

Twenty-eight apatite separates from 18 locations have been studied by the fission-track method following the methods of *Gleadow* [1984]. Irradiations were accomplished using the Oregon State University TRIGA reactor. Ages were calculated using a weighted-mean zeta calibration factor determined using Fish Canyon, Mt. Dromedary, and Durango standard apatites [*Miller et al.*, 1985]. Track density measurements were performed at a magnification of X1600, and confined-track-length measurements at X1563. Mean values of spontaneous to induced track densities ( $\rho_s/\rho_i$ ), rather than pooled ratios, were used to calculate ages and uncertainties where  $\chi^2 < 5\%$ . The closure temperature ( $T_c$ ) of fission tracks in apatite is taken to be  $100 \pm 10^\circ\text{C}$  [*Gleadow and Duddy*, 1981; *Harrison*, 1985; *Naeser et al.*, 1981; *Naeser and Faul*, 1969; *Wagner*, 1968]. The fission-track results are listed in Table 1. Uncertainties in the chronologic data are quoted at  $1\sigma$  unless otherwise stated.

## Results and Discussion

### Dazhuka Area

A mafic diorite (sample H4) was collected in the westernmost part of the study area, near the village of Dazhuka. The  $^{40}\text{Ar}/^{39}\text{Ar}$  results for hornblende and K-feldspar from this pluton are shown in Figure A1<sup>1</sup>.

The hornblende spectrum gives ages between 101 and 89 Ma over 83 % of the  $^{39}\text{Ar}$  released with a total gas age of 92.3 Ma. We take this to indicate that the rock cooled to  $\sim 500^\circ\text{C}$

between 90 and 100 Ma. This is consistent with a U-Pb zircon date from the same pluton of  $93.4 \pm 1.0$  Ma [*Schärer and Allègre*, 1984] but at variance with two previously reported  $^{40}\text{Ar}/^{39}\text{Ar}$  hornblende ages of 113 and 104 Ma [*Maluski et al.*, 1982]. It seems probable that the discrepancy between the hornblende ages of *Maluski et al.* [1982] and the concordant hornblende (this study) and zircon ages [*Schärer and Allègre*, 1984] is a possibly anomalously high ( $^{36}\text{Ar}/^{37}\text{Ar}$ )<sub>Ca</sub> correction factor used in that study. We conclude this pluton is no older than 95 Ma.

K-feldspar from this sample yields an age spectrum with two distinct ages, one in the range of  $\sim 42$  to 50 Ma and a second with an age of  $\sim 75$  Ma. The Arrhenius diagram for this sample suggests that it dwelled in the temperature range  $200$ – $250^\circ\text{C}$  during the interval 50 to 40 Ma.

### Nyemo Area

Eighty kilometers east of Dazhuka, near the village of Nyemo, a granodiorite was sampled at its contact with a pelitic gneiss. This sample, XR-2a, yielded separates of hornblende, biotite, and K-feldspar (Figure A2). The hornblende age spectrum is flat with an age over the last 30% of gas release of  $69.9 \pm 0.5$  Ma. The biotite spectrum is characterized by a narrow range of ages with an average of  $46.8 \pm 0.4$  Ma between 7 and 97%  $^{39}\text{Ar}$  released. The K-feldspar age spectrum is characterized by an initial portion (0–10%  $^{39}\text{Ar}$  released) with oscillating ages ranging down to  $\sim 10$  Ma, followed by a smooth increase in ages up to  $\sim 60$  Ma. These oscillations correspond to isothermal duplicate steps with the first step at a given temperature yielding both older ages and higher Cl/K (calculated from  $^{38}\text{Ar}/^{39}\text{Ar}$ ) ratios. It was recently discovered that a plot of the difference in age (implicitly  $\Delta^{40}\text{Ar}/\text{K}$ ) and Cl/K between the two isothermal steps commonly yields a linear array [*Harrison et al.*, 1993]. The slope of this line corresponds to the Cl-correlated composition of excess argon ( $^{40}\text{Ar}_E/\text{Cl}$ ) in the sample and can be used to correct for the contaminating argon. These results yield a well-correlated array over 3 orders of magnitude in  $\Delta\text{Cl}/\text{K}$  corresponding to a  $^{40}\text{Ar}_E/\text{Cl} = (1.45 \pm 0.04) \times 10^{-4}$ . Using this value, the results for the  $500^\circ$  to  $750^\circ\text{C}$  steps were corrected giving ages ranging from 6 to 11 Ma with an average of  $9.1 \pm 0.5$  (1 SE).

The K-feldspar age spectrum is well-fit using an essentially isothermal history ( $\sim 290$ – $270^\circ\text{C}$ ) from 60 to 9 Ma followed by rapid cooling at  $>100^\circ\text{C}/\text{m.y.}$  (Figure A3). This history is consistent with the nearby apatite age from sample PC-88-59 (Figure 2) of  $6.9 \pm 0.9$  Ma (Table 1).

The hornblende from sample XR-2a suggests that the pluton sampled near Nyemo has a crystallization age of probably not more than  $\sim 71$  Ma.

### Pachu Area

Two samples (PC-88-7 and PC-88-11) of a granodiorite pluton separated horizontally by 1 km were collected near the village of Pachu at elevations of 4145 and 4600 m, respectively. A third sample (PC-88-5) was collected along the road north of Pachu, approximately 8 km from the other samples at an elevation of 4140 m. The age spectra for biotite and K-feldspar from these three samples are shown in Figure A4.

The biotites are indistinguishable from one another with total gas ages of 14.1 Ma. The K-feldspars from these samples are also quite similar and only slightly younger than the

<sup>1</sup> Figures A1–A19 are listed in the Appendix and are available with the entire article on microfiche Order from American Geophysical Union, 2000 Florida Avenue, N.W., Washington, D.C., 20009. Document T94-002; \$2.50. Payment must accompany order.

biotites from the same samples. The results of forward modeling of the K-feldspars from sample PC-88-11 (Figure A5) are consistent with very rapid cooling at ~14 Ma. Assuming a cooling rates of ~100°C/m.y. and a diffusion lengthscale of 0.34 mm [Copeland *et al.*, 1987], a  $T_c$  of  $375 \pm 25^\circ\text{C}$  is calculated for the coexisting biotites. K-feldspar and biotite results from PC-88-5 are nearly identical. These thermal history results are consistent with a single cooling rate of 80°C/m.y. between 14.1 and 11.7 Ma for all these samples.

Apatite fission-track ages from sample PC-88-11 and PC-88-12 (along the same traverse as PC-88-11 and PC-88-7, taken at an elevation of 4200 m) are  $15.1 \pm 2.1$  and  $17.1 \pm 2.2$  Ma, respectively (Table 1). These results are both older than the coexisting biotites and have higher associated uncertainties. The thermal history results from the argon data suggest that temperatures approaching the thermal stability of fission tracks in apatite could not have been reached until after ~12 Ma. This is within the  $2\sigma$  uncertainties of PC-88-11 apatite, but outside that range for PC-88-12. Despite the possibility that spurious tracks may have been counted in one or both of these samples these results underscore the fact that this pluton must have experienced continued rapid cooling subsequent to 11.7 Ma.

At present, the time and depth of crystallization of the Pachu granodiorite are not known. The location, composition and texture of this pluton suggest that it is genetically similar to other Gangdese granitoids and is therefore older than 40 Ma. We therefore presume that the rapid cooling indicated by the  $^{40}\text{Ar}/^{39}\text{Ar}$  results from Pachu was not due to simple conductive cooling of a hot pluton adjacent to cold country rocks. During the middle Miocene these samples experienced rapid cooling. At elevated cooling rates the  $T_c$  for biotite is on the order of 340 to 380°C [see Harrison *et al.*, 1985]. PC-88-7 therefore cooled from ~70°C to ~200°C in the interval 14.2 Ma to 12.7 Ma. Samples PC-88-5 and PC-88-11 suggest slightly lower cooling rates in the time interval 14 to 12 Ma. The average cooling rate of these samples during the past 12 million years has been ~17 °C/m.y.

### Yangbajian Area

Three samples have been collected in or near the town of Yangbajian (Figure 2). One (PC-88-29, elevation 4300 m) from the lowest exposure of a coarse-grained granodiorite which intrudes quartzite and schist at elevations varying from 4600 to 4700 m. The second is a biotite-kyanite schist (PC-88-23, elevation 4890 m) from the country rocks of the granite. The third sample, a leucocratic biotite granite (PC-88-45, elevation 4400 m) which intrudes the granodiorite, was collected ~1 km NNW from PC-88-29. The age spectra for minerals from these samples are shown in Figure A6.

Previous geochronology from this area includes a U-Pb zircon age of ~50 Ma from a migmatitic granite; a biotite Rb-Sr age from the same samples gives an age of 49.0 Ma [Xu *et al.*, 1985]. Debon *et al.* [1986] report a similar Rb-Sr biotite age of 49.2 Ma from a granite in this general area.

Biotite from the kyanite schist has a  $^{40}\text{Ar}/^{39}\text{Ar}$  age spectrum which has ages between 48.3 and 50.0 Ma over 90% of the  $^{39}\text{Ar}$  released (Figure A6a). Sample PC-88-45, approximately 2 km to the west and 490 m lower in elevation, gives a similar age spectrum reflecting cooling through its  $T_c$  at

cairca 47 Ma (Figure A6b). The K-feldspar from this sample has an age gradient from 20 to 29 Ma over the first 25% of the  $^{39}\text{Ar}$  released followed by constant ages of 29 Ma over the remainder of the gas. Multi-diffusion-domain modeling of this sample is shown in Figure 3. This analysis suggests that the temperature to associate with these older ages is about 350°C. Therefore there must have been very little cooling from the time of closure of the biotite at 47 Ma to the time the largest domain began to retain argon at 29 Ma. At about this time, the sample experienced a rapid decrease in cooling to ~210°C at 28 Ma — this episode of cooling produced the flat segment of the age spectrum corresponding to the last 75% of the  $^{39}\text{Ar}$  released. The curved part of the age spectrum reflects slower cooling, to approximately 188°C at 20 Ma.

A low-K alkali feldspar from sample PC-88-29 has an irregular age spectrum with a total gas age of 39.6 Ma (Figure A6c). Apatite from this sample gives a fission-track age  $9.5 \pm 0.9$  Ma (Table 1) and may reflect accelerated cooling due to extension of the adjacent graben [Copeland and Harrison, 1993].

### Lhasa Region

Three separate plutons, the Lhasa granite, the Gu Rong granite, and the Dagze granite, have been investigated in the area near Lhasa (Figure 2).

**Gu Rong granite.** The Gu Rong granite is well exposed along the road from Lhasa to Yangbajian and contains abundant hornblende, biotite, and K-feldspar. The age spectra for these minerals from a sample (PC-88-39) collected at 3750 m, the base of the exposure, are given in Figure A7. These three minerals show a narrow range in age between 51 and 44 Ma; the bulk of the gas from the hornblende gives ages in the range 47 to 51 Ma; the biotite has a flat age spectrum at about 50 Ma; the K-feldspar has an age gradient from 44 to 48 Ma.

The total gas age for the biotite is 1.7 m.y. older than the total gas age for the hornblende. Although these two ages are not statistically different (at  $2\sigma$ ), the apparent reversal may represent non-atmospheric, trapped Ar in the biotite which cannot be resolved due to the high  $^{40}\text{Ar}^*/^{40}\text{Ar}_{\text{total}}$ . The  $^{40}\text{Ar}/^{39}\text{Ar}$  data for sample PC-88-39 strongly suggest that the Gu Rong granite was intruded at ~50 Ma and cooled to ~250°C within 5 m.y. The interpretation of these isotopic results (rapid cooling immediately after emplacement) is bolstered by the contact relations of this pluton; on the northwest side, on the road from Lhasa to Yangbajian the granite intrudes ignimbrites of the Linzizong Formation. These volcanic rocks are not regionally metamorphosed, and therefore the depth at which these units were originally juxtaposed must have been relatively shallow, promoting rapid cooling of hot magma against cold country rock.

Modeling of PC-88-39 K-feldspar (Figure A8) indicates that after the initial rapid cooling associated with cooling of magma against cold country rock the pluton stayed within a few degrees of 300°C for about 5 m.y. This almost isothermal segment of the cooling history is followed by an interval of extremely rapid cooling, closing the smallest domain in the feldspar at 44 Ma, when the rock reached ~180°C. This modeling is hampered, however, by the fact that it appears that the sample began to melt at about 38%  $^{39}\text{Ar}$  released. In such cases the details of the thermal history recorded by the most retentive portions of the mineral is obscured.

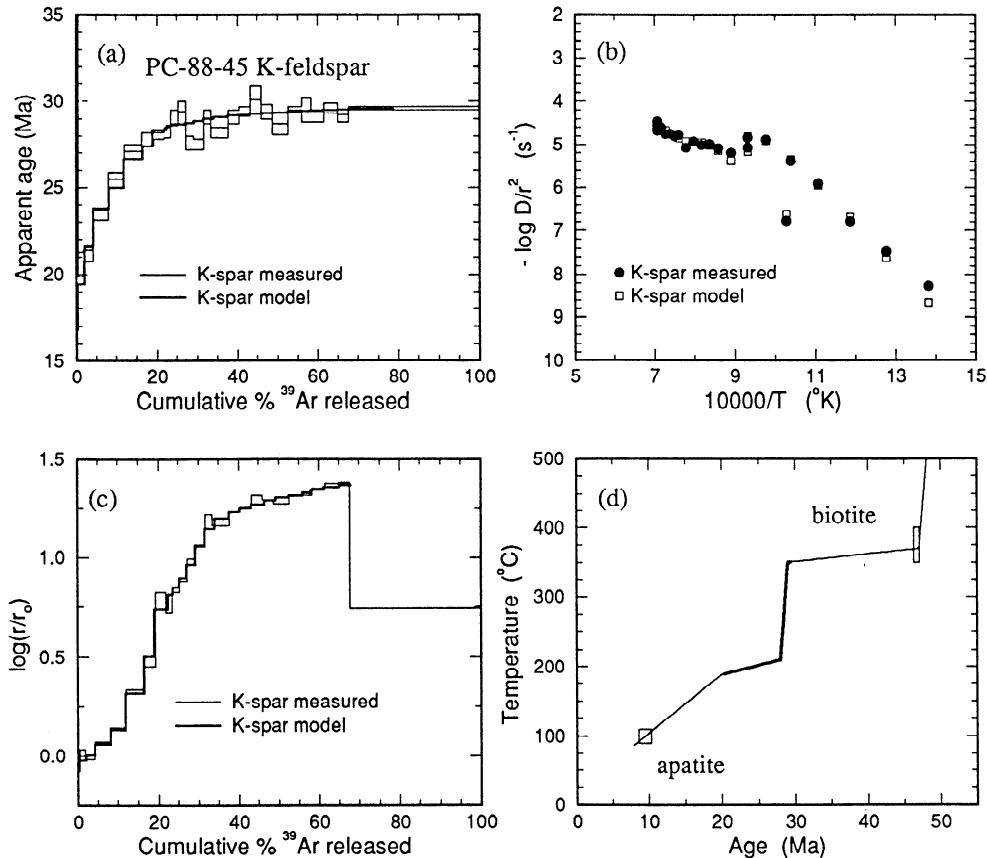


**Figure 3.** Results of multi-domain modeling of PC-88-45 K-feldspar. (a) age spectrum; (b) Arrhenius diagram for measured data (solid circles) and model (open squares) (c)  $\log(r/r_0)$  for data obtained from laboratory heating (thin line) and our model (thick line) which assumes 6 diffusion domains with an activation energy of 46.0 kcal/mole of relative sizes, 0.00138, 0.00526, 0.0128, 0.0635, 0.439, and 1.0 with volume fractions of 0.0079, 0.0599, 0.0894, 0.0797, 0.1246, and 0.6385, respectively. (d) Proposed thermal history which, based on the model from Figure 3c yields the model age spectra shown by the thick line in Figure 3a compared with the experimentally determined age spectra (thin lines). The portion of the cooling history constrained by the K-feldspar is given by the bold line in Figure 3d. The additional constraint of the biotite age from this sample is shown with a range of possible closure temperatures of 350–400°C.

Two apatite samples (PC-88-36, 4500 m elevation, and PC-88-39) from this pluton yield statistically indistinguishable ages of  $20.8 \pm 1.7$  and  $20.0 \pm 1.7$  Ma, respectively (Table 1). The second age is the average of two measurements of determinations from two irradiation packages. The similarity of the ages of these two samples which have a 750 m vertical separation suggests a second phase of rapid cooling at circa 20 Ma (Figure 4). The minimum denudation rate consistent with these data is 0.2 mm/yr but could have been much larger.

**Lhasa granite.** Three samples of the Lhasa granite were collected along a ~2-km long traverse at elevations of 4935 m, 4455 m, and 3720 m (samples K-88-40, K-88-42 and K-88-45, respectively). The age spectra for the five minerals analyzed from these samples are shown in Figure A9.

The biotites from the top and bottom of this 1215 m vertical traverse give irregular age spectra with total gas ages of 62.0 and 62.8 Ma. The three K-feldspars analyzed also yield similar results with age gradients beginning in the range 36 to 38 Ma and ending in ages of 48 to 50 Ma. The two concordant

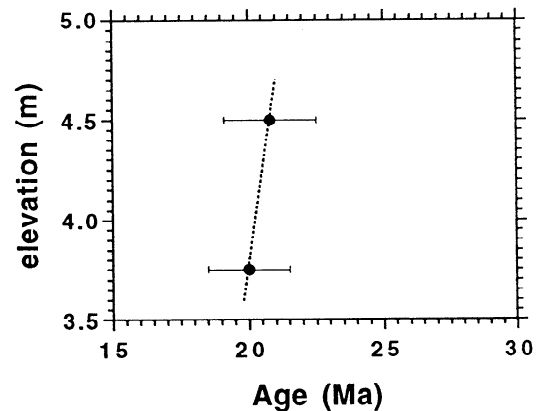


**Figure 4.** Apatite fission-track ages (Table 1) from the Gu Rong granite plotted elevation shown with  $1\sigma$  uncertainties. Dotted line shows probable history of the ~100°C isotherm (relative to present sea level) for this location.

biotite ages of  $62 \pm 1$  Ma from samples with a vertical separation of more than 1.2 km are older than the age inferred from U-Pb analysis of six zircon fractions of between 5 and 100 grains [Schärer and Allègre, 1984]. They plotted  $^{207}\text{Pb}/^{206}\text{Pb}$  versus  $^{238}\text{U}/^{206}\text{Pb}$  for these zircons and concluded that the Lhasa granite crystallized at  $\sim 53$  Ma and that the zircons in this body contained a component of inherited Pb\*. The biotite  $^{40}\text{Ar}/^{39}\text{Ar}$  ages are also older than two Rb-Sr biotite-whole rock isochrons from the Lhasa granite of 59.7 and 51.2 Ma [Debon *et al.*, 1986]. The apparent discrepancy between the biotite and zircon ages may be due to recent Pb\* loss from these zircons. Five of these six zircon fractions plot essentially on concordia, the sixth slightly to the right. These data can either be interpreted as the result of crystallization at some time since 50 Ma with an inherited component of Pb\* or as crystallization at some time before 59 Ma with subsequent Pb loss (with or without inherited Pb\*). This second scenario would suggest that the biotite  $^{40}\text{Ar}/^{39}\text{Ar}$  ages record a time close to the age of intrusion into cold country rock. An additional possibility is that the biotites contain equal amounts of excess Ar, and therefore the ages are not meaningful. Because this seems unlikely and the U-Pb zircon data do not clearly favor one interpretation over another, we infer that the Lhasa granite crystallized immediately prior to 62 Ma.

The Arrhenius relationships for these K-feldspar samples are suggestive of the presence of a very low volume fraction of a small domain. The practical consequence of this is that it is not possible to acquire detailed thermal history constraints with the same uncertainty as other data. The modeling for two of these samples is shown in Figures A10 and A11. In each of these samples we have taken the activation energy of Ar release from the high-temperature data, rather than the lower-temperature data, as is the more common practice.

The modeling of both of these feldspar samples suggests a phase of little cooling following closure of the biotite; apparently, the pluton did not move from its emplacement depth for  $\sim 25$  m.y. This was followed by a period of rapid cooling. As would be expected, the sample at the top of this mountain, K-88-40, shows evidence for this rapid cooling about 2 m.y. prior to sample K-88-45, 1250 m below. Although the sample at the top of the mountain appears to be hotter than the sample at the bottom of the mountain in the interval 46 to 40 Ma these results are not outside the general range of the uncertainty of this method and certainly not outside the range of these sample, whose Arrhenius plots are more difficult to interpret because of the apparent small proportion of a small domain and the large relative difference between the largest and smallest domains.

Apatite from sample K-88-45 gives a fission-track age of  $25.2 \pm 4.3$  Ma (Table 1). Thus it appears that the present exposure of the Lhasa granite maintained a temperature between  $\sim 150^\circ$  and  $120^\circ\text{C}$  between circa 37 and 25 Ma.

**Dagze granite.** Six minerals from two samples of the Dagze granite collected along a  $\sim 2$  km traverse were analyzed by  $^{40}\text{Ar}/^{39}\text{Ar}$  (Figure A12). These two samples, K-88-66 and K-88-72, were collected from the central portion of this pluton at 5050-m and 3970-m elevations, respectively. Another sample (M8-3), collected from the margin of this pluton, has been previously reported by Copeland *et al.* [1987]. The results from biotite and K-feldspar from this sample are essentially identical to K-88-66.

The hornblende, biotite, and K-feldspar from the top of this traverse (K-88-66) all yield maximum ages in their spectra in the range 55 to 57 Ma (Figure A12a). The first 40% of the  $^{39}\text{Ar}$  released from the K-feldspar yields an age gradient from 40 to 55 Ma. As with PC-88-39, the total gas age for the biotite is slightly older than the hornblende, but, again, the difference is not material to our interpretation. The  $^{40}\text{Ar}/^{39}\text{Ar}$  ages for these samples and the Arrhenius relationships for this K-feldspar suggest cooling from  $> 500^\circ\text{C}$  to  $275^\circ\text{C}$  in  $\sim 1$  m.y. at circa 55 Ma followed by cooling to  $\sim 220^\circ\text{C}$  by 40 Ma. The data from K-88-72, collected 1050 m below K-88-66, are essentially identical to K-88-66, although the K-feldspar from K-88-72 was analyzed in only a reconnaissance fashion (Figure A12b). In detail, the modeling of K-feldspar from sample K-88-66 indicates closure of the largest domains in the feldspar at circa 55 Ma and  $295^\circ\text{C}$  but almost no cooling in the intervening 10 m.y. Then, at  $\sim 44$  Ma, the sample experienced cooling at a rate of  $20^\circ\text{C}/\text{m.y.}$  to the closure of the smallest domain at 40 Ma and  $215^\circ\text{C}$  (Figure A13).

The sample from the top of this pluton gives an apatite fission-track age of  $33.3 \pm 5.2$  Ma; the lower sample, about 1 km below K-88-66, gives an age of  $19.1 \pm 2.1$  (Table 1, Figure A14). Assuming a geotherm of  $25\text{--}30^\circ\text{C}/\text{km}$ , these results give us a temperature-time datum for K-88-66 of  $19.1 \pm 2.1$  Ma at  $75 \pm 25^\circ\text{C}$ .

The rapid cooling from  $>500$  to  $\sim 295^\circ\text{C}$  at 55 Ma of a more than 1 km thick section of the Dagze granite suggests that this pluton crystallized at essentially this time.

### Quxu Pluton

The Quxu pluton is a composite pluton SW of Lhasa; Debon *et al.* (1986) have subdivided this pluton into five plutonic units based on geochemical and petrographic criteria. Samples from one phase of this pluton (unit A2) were investigated in earlier thermochronological studies [Copeland *et al.*, 1987; Richter *et al.*, 1991]. Additional samples were collected to investigate to what extent the rapid pulse of denudation beginning at circa 19 Ma reflected in the data from these earlier samples was recorded in other minerals of this pluton. Data from two additional sites are reported here; the first is a vertical traverse over some 800 m of elevation, the second site is a single sample collected near the village of Quxu. In addition, we report apatite fission-track ages from both the previous and new sites investigated by  $^{40}\text{Ar}/^{39}\text{Ar}$ .

Copeland *et al.* [1987] investigated five rock samples taken in a traverse from the northern part of this pluton with a vertical separation of 1000 m. Biotite  $^{40}\text{Ar}/^{39}\text{Ar}$  ages decrease monotonically with decreasing elevation from 26.8 to 17.8 Ma suggesting an increasing cooling rate through the biotite  $T_c$  over time. The similarity of the minimum  $^{40}\text{Ar}/^{39}\text{Ar}$  age from K-feldspars from all of these samples ( $\sim 17$  Ma) further indicates rapid cooling of the entire pluton at this time. Apatites from these same five samples yield ages that suggest a decrease in age from 16.4 Ma at the top to 15.0 Ma at the bottom (Figure 5), similar to the biotites, but, in fact, these ages are indistinguishable from one another at  $1\sigma$ . Fission-track distributions from three of these samples (top, middle, and bottom) are similar (Figure A15) with average track lengths of  $14.0 \pm 1.6$   $\mu\text{m}$ ,  $14.3 \pm 1.3$   $\mu\text{m}$ , and  $13.8 \pm 1.9$   $\mu\text{m}$ , respectively. This length distribution is characteristic of

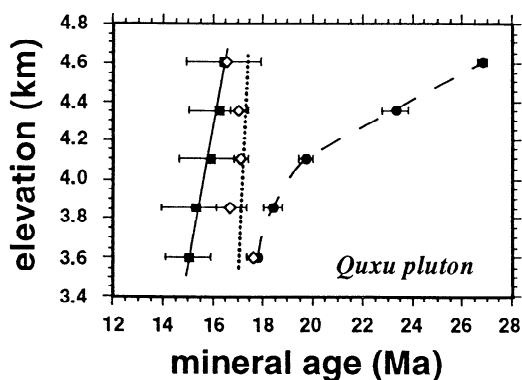


**Figure 5.** Shown are  $^{40}\text{Ar}/^{39}\text{Ar}$  biotite isochron ages (solid circle, dashed line indicates the history of the  $\sim 335^\circ\text{C}$  isotherm [Copeland *et al.*, 1987], relative to present sea level, for this location), minimum  $^{40}\text{Ar}/^{39}\text{Ar}$  K-feldspar ages (open diamond, dotted line indicates the history of the  $\sim 285^\circ\text{C}$  isotherm [Copeland *et al.*, 1987], relative to present sea level, for this location), and apatite fission-track ages (solid square, solid line indicates the history of the  $\sim 100^\circ\text{C}$  isotherm, relative to present sea level, for this location) from the Quxu granite plotted versus elevation shown with  $1\sigma$  uncertainties. Apatite data from Table 1; biotite and K-feldspar data from Copeland *et al.* [1987]. The relative poor fit of the K-feldspar data to the “best-fit line” may be due to complications with excess Ar in the early steps making it difficult to resolve the minimum age and/or a variability in the minimum closure temperature in these feldspars. Regardless of such minor complications, all of these data clearly show that this 1-km thick section of crust was brought towards the surface of the Earth extremely rapidly in the interval 19 to 15 Ma.

rapid cooling and further indicates a period of substantial denudation at this site in the interval 20 to 15 Ma.

One sample (H-88-1) was collected from the southernmost portion of the pluton, near the village of Quxu at an elevation of 3570 m (plutonic unit A2). Biotite from this sample yields a flat age spectrum at 42 Ma; K-feldspar shows a gradient in age from 26 to 42 Ma (Figure A16). Zircons from near this sample site have been dated by the U-Pb method at 41.4 Ma [Schärer and Allègre, 1984]. The concordance of the zircon, biotite, and the upper portion of the K-feldspar spectrum (Figure A16) indicates that this portion of the pluton was intruded into country rocks which were at a temperature of  $\sim 300^\circ\text{C}$  at 42 Ma. Modeling of H-88-1 K-feldspar (Figure A17) yields a cooling history characterized by moderate cooling rates through the  $T_c$  of the largest domain ( $\sim 275^\circ\text{C}$ ) down to about  $215^\circ\text{C}$  at 27 Ma followed by an accelerated cooling to  $155^\circ\text{C}$  at 25.5 Ma.

Samples H-88-1 and H-88-2 (collected from the same area) yield apatite fission-track ages of  $18.6 \pm 1.5$  and  $21.4 \pm 2.9$  Ma, respectively. The length distribution of fission tracks in apatites from sample H-88-1 (Figure A15d) indicates rapid cooling at this time. Sample K-88-73, collected across the Tsangpo River from these samples, has a similar apatite fission-track age of  $20.2 \pm 1.6$  Ma (Table 1).

Two samples, PC-88-30 and PC-88-32, were collected at elevations of 3760 m and 4560 m, respectively,  $\sim 10$  km to the

SSW of the sample traverse described in Copeland *et al.* [1987] (Figure 2). These two samples correspond to plutonic unit D of Debon *et al.* [1986]. The hornblende from the lower sample yields a reasonably flat age spectrum over more than 90% of the  $^{39}\text{Ar}$  released with ages of about 49 Ma; K-feldspar from this sample shows a minimum age of  $\sim 19$  Ma at  $\sim 20\%$  of the  $^{39}\text{Ar}$  released followed by an increase to ages of  $\sim 27$  Ma (Figure 6a). Biotite from the upper sample yields a flat age spectrum with an age of  $\sim 38$  Ma (Figure 21c).

Modeling of sample PC-88-30 (Figure 7) yields a cooling history which is characterized by three segments: the first cooling from  $355^\circ\text{C}$  to  $305^\circ\text{C}$  in the interval 27.7 to 25.0 Ma, the second cooling from  $305^\circ\text{C}$  to  $295^\circ\text{C}$  from 25.0 to 19.8 Ma, and the third an interval of more rapid cooling to  $\sim 200^\circ\text{C}$  by 19.6 Ma.

Biotite from sample PC-88-32 yields a  $^{40}\text{Ar}/^{39}\text{Ar}$  age of  $\sim 38$  Ma (Figure 6b). K-feldspar from this sample has been described in detail by Richter *et al.* [1991]. They found that the age spectrum was consistent with a thermal history similar in form to that of the model age spectrum for PC-88-30 presented in Figure 7d. The difference in these thermal histories is a consequence of the elevation at which these samples were collected. The dashed line in Figure 7d shows the model cooling curve for PC-88-32 which was collected 800 vertical meters above PC-88-30. The difference in these two curves of  $\sim 30^\circ\text{C}$  from 26 to 20 Ma allows a direct calculation of a paleogeothermal gradient during this interval of  $\sim 38^\circ\text{C}/\text{km}$ . This elevated value is consistent with subduction-related magma-

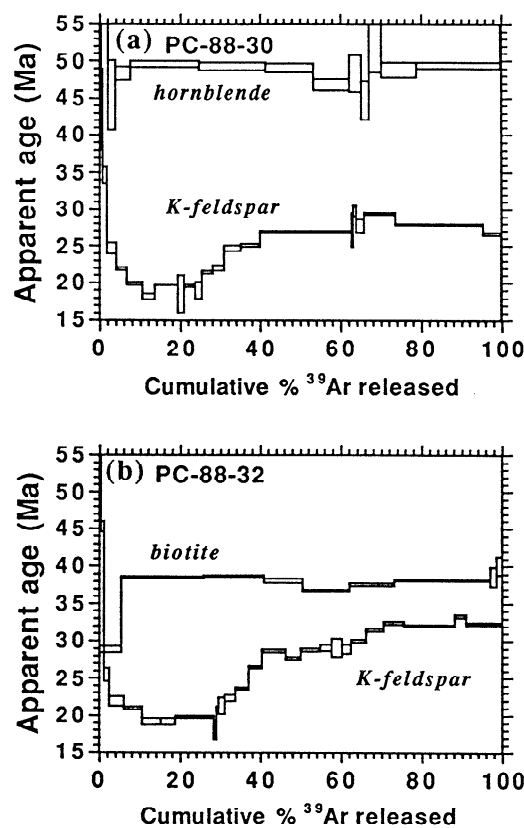


**Figure 6.**  $^{40}\text{Ar}/^{39}\text{Ar}$  age spectra samples taken from the near Quxu (Figure 2). (a) PC-88-30. (b) PC-88-32.



## PC-88-30 K-feldspar

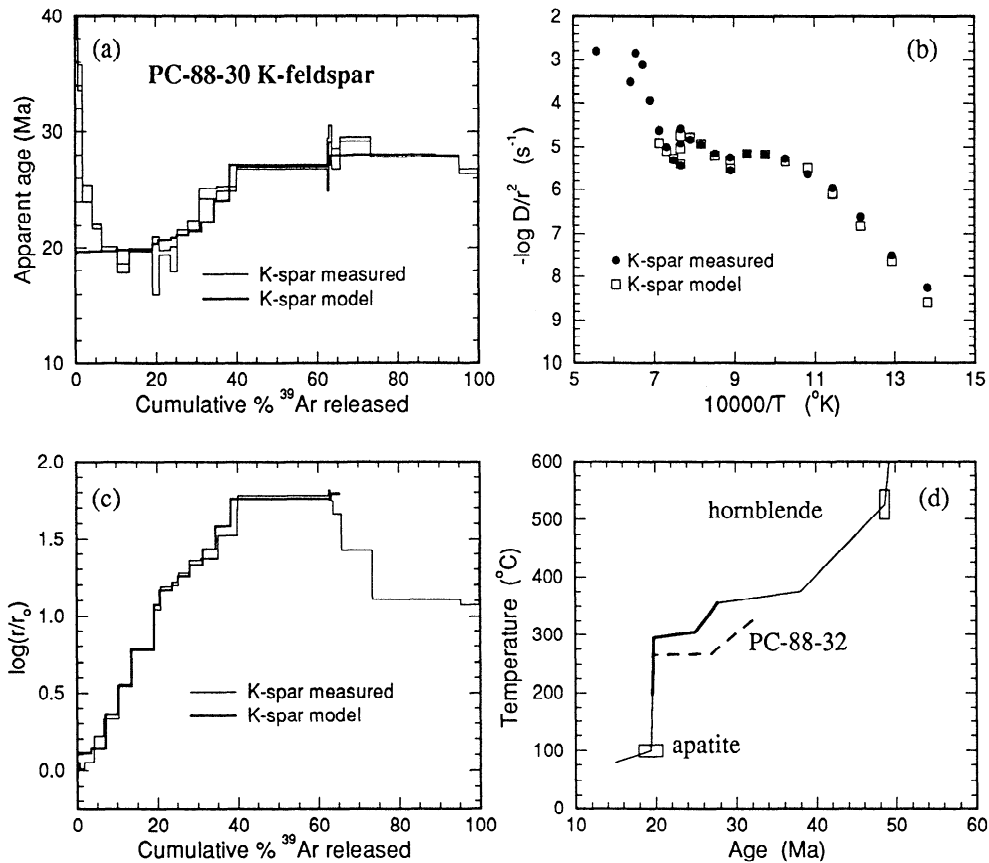


**Figure 7.** Results of multi-domain modeling of PC-88-30 K-feldspar. (a) Age spectrum; (b) Arrhenius diagram for measured data (solid circles) and model (open squares). (c)  $\log(r/r_0)$  for data obtained from laboratory heating (thin line) and our model (thick line) which assumes 4 diffusion domains with an activation energy of 48.2 kcal/mole of relative sizes, 0.00178, 0.00959, 0.0804, and 1.0 with volume fractions of 0.0645, 0.0972, 0.1230, and 0.7153, respectively. (d) Cooling history which, based on the model from Figure 7c yield the model age spectra shown by the thick line in Figure 7a compared with the experimentally determined age spectra (thin lines). The part of the cooling history constrained by the K-feldspar is given by the heavy line in Figure 7d. The dotted line in Figure 7d is from a nearby sample (PC-88-32), previously reported by Richter *et al.* (1991). The difference in elevation of these two samples (~800 m) allows determination of a paleogeothermal gradient at this location; we calculate a value of ~38°C/km during the interval 26 to 20 Ma.

tism having ceased only ~14 million years prior to this period.

### Samye Area

A sample of tonalite (PC-88-65) was collected approximately 6 km west of the village of Samye at an elevation of 3750 m. The <sup>40</sup>Ar/<sup>39</sup>Ar age spectra for hornblende and biotite from this sample are shown in Figure A18. The hornblende exhibits a “plateau” over 76% of the <sup>39</sup>Ar released with ages in the range 72 to 65 Ma. The first part of the gas released gives younger ages. These ages are associated with much lower <sup>37</sup>Ar/<sup>39</sup>Ar values, suggesting a small component of biotite in this hornblende separate. Biotite from this sample gives ages of ~48 Ma over the last 75% of <sup>39</sup>Ar released.

The precise time of crystallization of the Samye tonalite is less well constrained, but since our <sup>40</sup>Ar/<sup>39</sup>Ar dating of hornblende elsewhere in the Gangdese batholith seems generally to

give near-crystallization ages, we estimate the age of the Samye tonalite to be ~68 Ma.

Two samples from this pluton have been analyzed for apatite fission-track ages. Sample PC-88-62, collected at an elevation of 4440 m, gives an age of  $27.5 \pm 3.3$  Ma; PC-88-65 (3750 m) gives an age of  $24.9 \pm 2.3$  Ma (Table 1). These data are shown in Figure A19 and indicate cooling of this pluton below ~100°C in the late Oligocene to early Miocene but the higher uncertainties make determination of the rate of cooling more difficult.

### Conclusions

#### Timing of Magmatism in the Gangdese Batholith

This study confirms three previously published ages, suggests the revision of one published age, and presents estimates on the age of crystallization for four additional plutons.

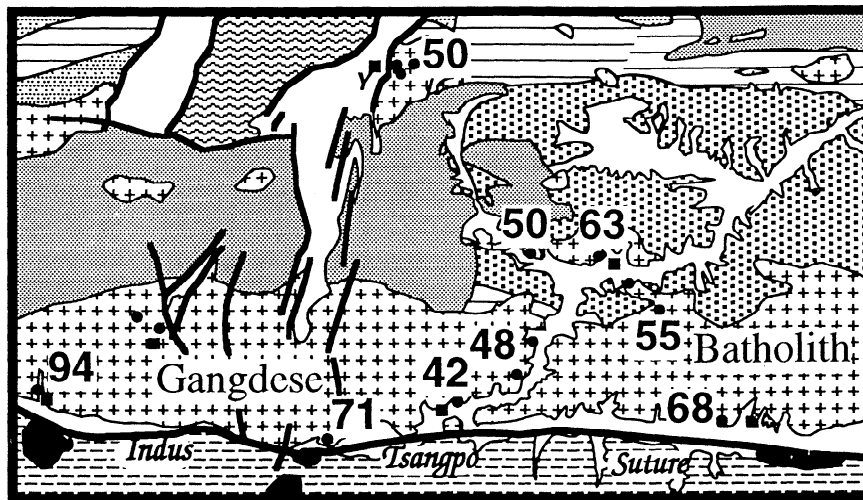


Figure 8. Map of study area showing estimated time of emplacement of plutons studied (in Ma).

Figure 8 shows the geographic distribution of the presently available crystallization ages for plutons of the Gangdese batholith in the Lhasa area.

The previously reported U-Pb ages for the Dazhuka diorite [Schärer and Allègre, 1984] and the granite at Yangbajian [Xu *et al.*, 1985] are essentially identical to the oldest  $^{40}\text{Ar}/^{39}\text{Ar}$  age from these plutons reported here, suggesting the  $^{40}\text{Ar}/^{39}\text{Ar}$  hornblende age is a good approximation for the crystallization age of the plutons in the eastern Gangdese. A similar confirmation of the age of the southern part of the Quxu pluton is given by the concordance of the U-Pb zircon age [Schärer and Allègre, 1984] and the  $^{40}\text{Ar}/^{39}\text{Ar}$  biotite age in sample H-88-1. However, the other two parts of this pluton suggest slightly older crystallization ages: the hornblende from sample PC-88-30 has an age of ~50 Ma, and the four hornblendes collected ~10 km to the northeast have an average age of 43.5 Ma [Copeland *et al.*, 1987]. These data suggest that despite chemical and mineralogical similarities [Debon *et al.*, 1986] the rocks of the "Quxu pluton" were intruded as at least two (and probably three or more) separate plutons over a period of at least 8 m.y.

The Lhasa and Gu Rong granites have been referred to as the "Lhasa-Gu Rong granite" by some workers [e.g., Debon *et al.*, 1986; Harris *et al.*, 1988b]. While some differences exist between these two plutons (the Gu Rong has much more abundant hornblende), in the absence of any precise chronologic data for the two bodies, their proximity to one another would be reasonable justification for grouping the two together. Available Rb-Sr ages from these two granites are similar but are only two-point isochrons [Debon *et al.*, 1986]. The  $^{40}\text{Ar}/^{39}\text{Ar}$  data presented here suggest that the Lhasa and Gu Rong plutons are separate units which crystallized at ~63 and ~50 Ma, respectively.

The range of crystallization ages for plutons in the Gangdese batholith has been established to be 120 to 40 Ma [Harris *et al.*, 1988a]. The available data from throughout the Gangdese batholith show that there have been two distinct periods of plutonism within the area ~100 km north of the Indus-Tsangpo suture — broadly 120 to 90 Ma and 70 to 40 Ma. Except for the Dazhuka diorite (and perhaps the Pachu

granite) all the granitoids studied in the Lhasa area fall within the younger group. The paucity of evidence for Gangdese plutonism in the interval 90 to 70 Ma may reflect shallow subduction of oceanic crust beneath the Lhasa terrane at this time. An  $^{40}\text{Ar}/^{39}\text{Ar}$  biotite age of  $76.6 \pm 1.5$  Ma from an andesite near Amdo [Coulon *et al.*, 1986], ~300 km north of Lhasa, is consistent with this interpretation. The large proportion of ages from 55 to 40 Ma in the Gangdese batholith suggests that subduction was steeper during the Eocene. Such a geometry might be expected, as the oceanic crust being subducted at that time, closest to the Indian passive margin, was likely relatively old and cold and would have tended to sink rapidly.

#### Tectonic Implications

Assuming a geothermal gradient of  $30^\circ\text{C}/\text{km}$ , the average post-40 Ma denudation rates calculated for the plutonic rocks in the study area vary from 0.18 to 0.30 mm/a. It is not clear, however, to what extent this rather narrow range of values is representative of the entire region shown in Figure 2. The Late Cretaceous-early Tertiary sedimentary and volcanic rocks in the region (shaded areas and solid squares in Figure 2) appear not to have been buried to depths greater than ~6 km; these rocks are virtually devoid of any metamorphic overprint, and concordant biotite and sanidine  $^{40}\text{Ar}/^{39}\text{Ar}$  ages of ~50 Ma have been reported from a trachyte near Yangbajian [Coulon *et al.*, 1986]. This implies tilting and shuffling of small blocks of crust of the southern Tibetan plateau since the collision began. For example, the contact between the Gu Rong granite and the volcanic rocks to the north is clearly intrusive. However, K-feldspars from three ignimbrites from the Maqu area have  $^{40}\text{Ar}/^{39}\text{Ar}$  age spectra with age gradients from ~55 to 40 Ma, suggesting slow cooling due to burial after eruption and subsequent erosion [Pan, 1993]. While there is no other suggestion of burial of the ignimbrites in the Maqu area to depths >6-8 km in the early Eocene, it is not unreasonable to believe that such basins may have existed in a local extensional regime in the Gangdese volcanic arc at this time. Much more work is needed to establish the details of the erosion histories of various sites in southern Tibet and the relative differences between the plutonic and stratified rocks. As shown

from this and other work, results from  $^{40}\text{Ar}/^{39}\text{Ar}$  analysis of K-feldspars can provide some important constraints in some places and little to no information in others. However, in those areas where K-feldspar analysis does not provide a clear picture, apatite fission-track analysis may. A particularly good example of this comes from the Dagze pluton where only the apatite data reveal, perhaps, the tectonically most significant interval, the episode of rapid cooling at ~20 Ma.

In every pluton studied, except the Pachu, any early cooling associated with the placement of a hot pluton against colder country rock can be distinguished from subsequent changes in cooling rate related to some younger tectonic process. Such cooling is most likely related to rapid denudation of the overlying rocks due to one of two processes (1) thinning of the overburden via extension faulting or (2) rapid erosion of the overburden due to the establishment and maintenance of steep topography in response to crustal thickening and isostatic adjustment. While both of these processes imply rapid movement of a sample toward the surface of the Earth, they may have distinctly different implications regarding movement relative to an external reference, such as sea level. In the first instance, the motion of a sample relative to present sea level could be zero or, perhaps, even negative. In the latter case, the motions relative to the surface of the Earth and relative to the geoid are both positive, although not simultaneous. The rapid erosion will not occur until after steep positive topography is present. Therefore, whereas the rapid cooling reflected in mineral ages from a sample from an extensional environment will essentially date the tectonic event responsible for the cooling, the cooling of a sample caused by erosion following uplift due to isostatic compensation of a thickened crust will lag behind the crustal thickening.

Normal faulting does not appear to have significantly modified the Gangdese batholith in the study area at the various times of rapid cooling revealed by the data presented here. A large shallow-dipping (5 to 20°), down-to-the-north normal fault zone has been recognized in the High Himalaya, ~150 to 200 km south of the Gangdese batholith [Burchfiel and Royden, 1985; Burg et al., 1984]. This zone was active in the Mt. Everest area between 22 and 19 Ma and perhaps as recently as early Pliocene a few tens of kilometers to the north [Burchfiel et al., 1992]. However, this fault zone is too far away to have any effect on the Miocene cooling history of the Gangdese batholith. East-west extension due to normal faulting along the Yadong-Gulu rift, which cuts the batholith in the region of Pachu and Nyemo, can be constrained to be at least as old as 5 Ma but not likely more than 10 Ma [Mercier et al., 1987; Harrison et al., 1992, 1993]. Therefore it seems that the dominant mechanism responsible for the rapid cooling since 40 Ma is rapid erosion of recently developed steep topography.

The Quxu results have been interpreted as the result of uplift (relative to sea level), followed by rapid erosion at circa 20 Ma [Copeland et al., 1987; Richter et al., 1991]. The samples at Pachu suggest a similar event affected this part of the batholith at ~15 Ma. Presuming that the Pachu pluton is older than the initiation of the collision between India and Asia, the cooling rate of 80°C/m.y. suggests that from 14 to 13 Ma, between 2 and 2.5 km of material was removed from the Pachu granite. In order to maintain such rapid erosion for over 1

m.y., local uplift (relative to sea level) must have at least kept up with erosion. Therefore uplift in this part of southern Tibet was occurring at a rate greater than ~2 mm/year in the interval of ~15 to 13 Ma. Further work on these samples (apatite fission-track,  $^{40}\text{Ar}/^{39}\text{Ar}$  hornblende, and U-Pb zircon dating, and hornblende geobarometry) is needed to more precisely define the tectonic history here.

The data from the two plutons near Yangbajian do not clearly define a steep segment on the cooling curve in Figure 3 similar to the Quxu and Pachu plutons but the long period of relatively slow cooling from 29 to 20 Ma and the fact that this region was at a temperature of ~200 °C as recently as 20 Ma suggest a period of more rapid cooling since 20 Ma. The  $T_c$  of the small diffusion domains in the K-feldspar suggest an average denudation rate for this area of 0.33 mm/yr since 20 Ma. It seems unlikely that this average rate was maintained throughout this period, so a brief pulse of denudation of up to 2 mm/yr in the interval of 20 to 5 Ma is probable. It is not clear whether this denudation is due to a pulse of uplift similar to that inferred for the Quxu and Pachu areas or is due to the extension in the Yangbajian graben.

We have previously speculated that rapid denudation of the Gangdese batholith in the Lhasa region is due to motion on the Gangdese thrust system (GTS), a north-dipping, south-directed system active during the mid-Tertiary [Harrison et al., 1992]. This feature, observed 40 km east of the study area at Zedong but probably obscured from view between Quxu and Samye by the Rinbung-Zedong thrust (RZT) [Yin et al., 1994], may provide the key to understanding the similarities and distinctions among the thermal histories estimated in this study.

Near Zedong, Yin et al. (1994) documented a >200 m thick north-dipping shear zone that juxtaposes the southern margin of the Gangdese batholith on top of deformed Tethyan sediments. Kinematic indicators and geological relationships clearly indicate that this fault is a south-directed thrust. Thermochronometry of samples in the shear zone and undeformed hanging wall constrain initiation of motion up the thrust ramp to be  $27 \pm 1$  Ma. Assuming that thrusting proceeded at a rate similar to the present convergence in the Himalaya (~18 mm/yr), the tip of the footwall bend would have reached the northern margin of the Gangdese batholith by ~22 Ma (Figure 9). Thus, we attribute the general younging to the north of minimum K-feldspar ages and apatite fission-track ages in the eastern part of our field area to movement of material south along the thrust, reaching the deepest part of the footwall ramp and moving closer to the surface.

Farther to the west, in the vicinity of Nyemo, the southern margin of the batholith is juxtaposed against the Xigaze Group, a Late Cretaceous to Paleogene sequence of forearc deposits, along a north-directed thrust. The fault contact is interpreted to be part of a pop-up structure that marks the Gangdese thrust system west of Nyemo [Yin et al., 1994]. From cross-cutting relationships, motion on this fault had terminated by 18 Ma.

These two manifestations of the GTS in the study area suggest that segments of the Gangdese batholith will have experienced different crustal thickening regimes and thus have different uplift and denudation histories. On the basis of this model we suggest that the GTS was the dominant mechanism responsible for cooling the contiguous portion of the

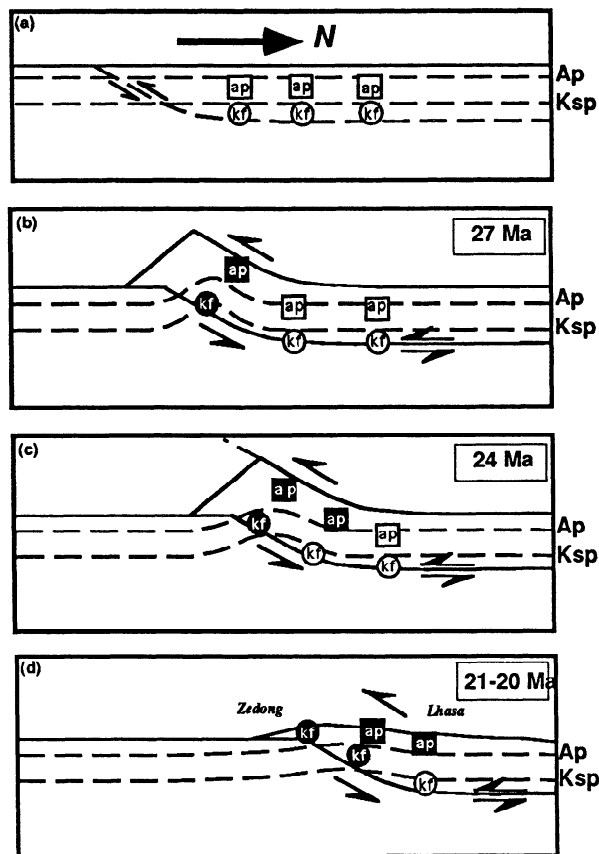


**Figure 9.** Schematic representation of the evolution of the Gangdese thrust system [see Yin *et al.*, 1994] and its influence on the thermochronology of the region. (a) Orientation of the K-spar closure isotherm for Ar diffusion ( $\sim 200^\circ\text{C}$ ) and the isotherm for annealing of fission tracks in apatite ( $\sim 100^\circ\text{C}$ ), (dashed lines), prior to movement of the Gangdese Thrust (solid line). In this and subsequent panels, white symbols with black lettering represent a sample above a particular closure temperature (ap=apatite, kf=K-feldspar); white on black represents a sample below the appropriate closure temperature. At 27 Ma (Figure 9b), the Gangdese Thrust starts to move, bringing the southern-most samples toward the surface of the Earth, turning on the thermochronologic clocks in these minerals. As time progresses, material is moved southward along the thrust and up the footwall ramp, causing an apparent northward progression of the closure isotherms. Note that material depicted in Figures 9a and 9b has been removed by erosion by the bottom panel. Such a scenario is consistent with the experimentally derived thermal histories of the Gangdese batholith in the eastern part of the study area; mineral ages for K-feldspar and apatite becoming older to the north.

batholith east of the disappearance of the Xigaze Group beneath the RZT. West of this point, the relationship between the GTS and crustal thickening in the batholith is less clear owing to the pop-up structure accommodating its movement. The cooling histories of the granitoids from Yangbajian, Pachu, and Nyemo may further be complicated by opening of the Yadong-Gulu rift in which they are sited.

Thermochronometry from the rectangular block defined by H-88-1 (Quxu) and PC-88-65 (Samye) on the southwestern and southeastern edges, respectively, and PC-88-39 and K-88-40 on the northern edge appear broadly consistent with the history of thrusting proposed by Yin *et al.* [1994].

We earlier emphasized the role of erosional and tectonic denudation in cooling rocks of the middle crust. An additional process introduced by the GTS hypothesis is cooling due to thrusting cold rock beneath hot. We envision three post-40-Ma thermal regimes in the hanging wall of the GT (1) a zone adjacent the thrust surface extending out a distance corresponding to a conductive timescale of up to  $\sim 5$  m.y. (i.e., the inferred duration of thrusting) in which the thermal evolution is dominated by cooling from below (note that because arrival of the a point on the hanging wall at the base of the ramp is diachronous, this lengthscale will vary from  $\sim 10$  km across in the south to  $\sim 5$  km across in the northern Gangdese); (2) a regime sufficiently far from the thrust surface in which cooling is dominated by erosional denudation in response to thrust-related crustal thickening; and (3) a transition region between regimes 1 and 2. In regime 1 we see evidence for early rapid cooling from both samples H-88-1 and PC-88-65. The K-feldspar results from Quxu and the apatite fission track ages from Samye show onset of rapid cooling at circa 26 Ma. Although indicating very different amounts of subsequent denudation, this age is similar to estimated time of initiation of the GTS of 27 Ma [Yin *et al.*, 1994].

Fission-track data from the northern Gangdese batholith, specifically, the Gu Rong and Lhasa granites, indicate a transition from a low to high denudation rate at  $\sim 21$  Ma. Given that the lag between establishing high topography due to crustal thickening and effecting cooling at depths of  $\sim 4$ -5 km is probably on the order of  $\sim 1$ -2 m.y., this implies that the northern edge of the thrust reached the Lhasa area by  $\sim 21$ -23 Ma. The relatively small amount of late Oligocene-early Miocene overburden removal ( $\sim 4$  km) in the northern part of the belt compared with the central and southern portions (typically, 10-12 km) suggests that a wedge-shaped thrust would not have penetrated much farther north than the Lhasa region. Interpreted in this way, these results appear to be consistent with initiation of the GTS a few tens of km south of the present Tsangpo river at 27 Ma and continued movement northwards at a rate of  $20 \pm 10$  mm/yr until  $\sim 22$  Ma [Yin *et al.*, 1994].

There are six clear examples of post-40-Ma rapid cooling: the Quxu, Pachu, Gu Rong, Dagze, and Nyemo plutons and the area around Yangbajian. The last two of these experienced rapid periods of cooling at circa 9 and 29 Ma, respectively (Figures A3, 3), whereas all the others experienced a brief period of extremely rapid erosion sometime in the interval of 26 to 15 Ma. The results from the Samye area, due to their greater uncertainty, are more equivocal but also suggest a brief acceleration of erosion in the late Oligocene or early Miocene.

One of the fundamental questions regarding the geology of Asia is how the Tibetan plateau attained its present great thickness, approximately double that of normal continental crust. The data presented here do not favor models in which the southern Tibetan plateau is progressively thickened and uplifted at a constant rate [e.g., Zhao and Morgan, 1985] or very late in the collisional history [e.g., Powell, 1986]. On

the basis of the remarkably flat present-day topography of the Tibetan plateau, *Fielding et al.* [1994] suggested that only models such as continental-scale underthrusting [e.g., *Barazangi and Ni*, 1982] or injection into the lower crust [*Zhao and Morgan*, 1985] could achieve the present situation of a large, relatively flat plateau. While we are greatly aided by the modern geophysical measurements in a still-active orogen, such as the Himalaya-Tibet system, these data permit relatively little evolutionary insight into the evidence left in the rock record. All available geological and geochemical data from the greater Lhasa area favor models in which the southern Tibetan plateau is thickened by distributed shortening [e.g., *Dewey and Burke*, 1973]; the Gangdese Thrust System [*Yin et al.*, 1994] may have been one of the important structures

accommodating convergence between India and Asia in this region during the late Oligocene to early Miocene.

**Acknowledgments.** We wish to thank Xie Yinwei for assistance in the field, Zhu Bingquan for general expediting of our 1988 expedition within China and Tibet, An Yin for discussions of Tibetan tectonics, Rick Ryerson for Figure 9 and sample XR-2a, and Matt Heizler for assistance with the  $^{40}\text{Ar}/^{39}\text{Ar}$  analyses. We benefited from reviews by Kevin Burke, Mike Searle, Kip Hodges, and an anonymous reviewer. This research was financially supported by U.S. National Science Foundation grants EAR-9118125, EAR-9118126, and EAR-9118127, and Academia Sinica

## References

- Barazangi, M., and J. Ni, Velocities and propagation characteristics of Pn and Sn beneath the Himalayan arc and Tibetan plateau: Possible evidence for underthrusting of Indian continental lithosphere beneath Tibet, *Geology*, *10*, 179-185, 1982.
- Burchfiel, B.C. and L.H. Royden, North-south extension within the convergent Himalayan region, *Geology*, *13*, 679-682, 1985.
- Burchfiel, B.C., C. Zhiliang, K.V. Hodges, L. Yuping, L.H. Royden, D. Changrong, and X. Jiene, The South Tibetan Detachment System, Himalayan orogen: Extension contemporaneous with and parallel to shortening in a collisional mountain belt, *Special Paper Geol. Soc. Am.* 269, 48 pp., 1992.
- Burg, J.P., M. Brunel, D. Gapais, G.M. Chen, and G.H. Lin, Deformation of leucogranites of the crystalline Main Central Sheet in southern Tibet (China), *J. Struct. Geol.*, *6*, 535-542, 1984.
- Copeland, P., Cenozoic tectonic evolution of the southern Tibetan plateau and eastern Himalaya: Evidence from  $^{40}\text{Ar}/^{39}\text{Ar}$  dating, Ph.D. dissertation, 414 pp., State Univ. of N.Y. at Albany, 1990.
- Copeland, P., and T.M. Harrison, The Nyainqentanghla range, southern Tibet: timing of the attainment of a large, high plateau and implications for development of the Asian monsoon, *Geol. Soc. Am. Abstr. Programs*, *25*, A175, 1993.
- Copeland, P., T.M. Harrison, W.S.F. Kidd, X. Ronghua, and Z. Yuquan, Rapid early Miocene acceleration of uplift in the Gangdese Belt, Xizang-southern Tibet, and its bearing on accommodation mechanisms of the India-Asia collision, *Earth Planet. Sci. Lett.*, *86*, 240-252, 1987.
- Coulon, C., H. Maluski, C. Bollinger, and W. S., Mesozoic and Cenozoic volcanic rocks from central and southern Tibet:  $^{39}\text{Ar}/^{40}\text{Ar}$  dating, petrological characteristics and geodynamical significance, *Earth Planet. Sci. Lett.*, *79*, 281-302, 1986.
- Debon, F., P. Le Fort, S.M.F. Sheppard, and J. Sonet, The four plutonic belts of the Transhimalaya - Himalaya: a chemical, mineralogical, isotopic, and chronological synthesis along a Tibet - Nepal section, *J. Petrol.*, *21*, 219-250, 1986.
- Dewey, J.F., and J.M. Bird, Mountain belts and the new global tectonics, *J. Geophys. Res.*, *75*, 2625-2647, 1970.
- Dewey, J.F., and K. Burke, Tibetan, Variscan and Precambrian basement reactivation: products of continental collision, *J. Geol.*, *81*, 683-692, 1973.
- Fielding, E., B. Isacks, M. Barazangi, and C. Duncan, How flat is Tibet?, *Geology*, *22*, 163-167, 1994.
- FitzGerald, J. and T.M. Harrison, Argon diffusion domains in K-feldspar I: microstructures in MH-10, *Contrib. Mineral. Petrol.*, *113*, 367-380, 1993.
- Gleadow, A.J.W., Fission-track dating method II: A manual of principles and techniques, in Workshop of Fission-Track Analysis: Principles and Applications, James Cook University, Townsville, Queensland, Australia, 1984.
- Gleadow, A.J.W. and I.R. Duddy, A natural long-term annealing experiment for apatite, *Nucl. Tracks*, *5*, 169-174, 1981.
- Harris, N.B.W., X. Ronghua, C.L. Lewis, and J. Chengwei, Plutonic rocks of the 1985 Tibet Geotraverse, Lhasa to Golmud, *Philos. Trans. R. Soc. London*, *A327*, 145-168, 1988a.
- Harris, N.B.W., X. Ronghua, C.L. Lewis, C.J. Hawkesworth, and Z. Yuquan, Isotope geochemistry of the 1985 Tibet Geotraverse, Lhasa to Golmud, *Philos. Trans. R. Soc. London*, *A327*, 263-285, 1988b.
- Harrison, T.M., Diffusion of  $^{40}\text{Ar}$  in hornblende, *Contrib. Mineral. Petrol.*, *78*, 324-331, 1981.
- Harrison, T.M., A reassessment of fission-track annealing behavior in apatite, *Nucl. Tracks*, *10*, 329-333, 1985.
- Harrison, T.M., and J.D. FitzGerald, Exsolution in hornblende and its consequences for  $^{40}\text{Ar}/^{39}\text{Ar}$  age spectra and closure temperature, *Geochim. Cosmochim. Acta*, *50*, 247-253, 1986.
- Harrison, T.M., and I. McDougall, Excess  $^{40}\text{Ar}$  in metamorphic rocks from Broken Hill, New South Wales: implications for  $^{40}\text{Ar}/^{39}\text{Ar}$  age spectra and the thermal history of the area, *Earth Planet. Sci. Lett.*, *55*, 123-149, 1981.
- Harrison, T.M., I.J. Duncan, and I. McDougall, Diffusion of  $^{40}\text{Ar}$  in biotite: Temperature, pressure and compositional effects, *Geochim. Cosmochim. Acta*, *49*, 2461-2468, 1985.
- Harrison, T.M., P. Copeland, W.S.F. Kidd, and A. Yin, Raising Tibet, *Science*, *255*, 1663-1670, 1992.
- Harrison, T.M., M.T. Heizler, and O.M. Lovera, 1993, In vacuo crushing experiments and K-feldspar thermochronometry, *Earth Planet. Sci. Lett.*, *117*, 169-180, 1993.
- Kidd, W.S.F., Y. Pan, C. Chang, M.P. Coward, J.F. Dewey, A. Gansser, P. Molnar, R.M. Shackleton, and Y. Sun, Geological mapping of the 1985 Chinese-British Tibetan (Xizang-Qinghai) Plateau Geotraverse route, *Philos. Trans. R. Soc. London*, *A327*, 287-305, 1988.
- Lovera, O.M., F.M. Richter, and T.M. Harrison,  $^{40}\text{Ar}/^{39}\text{Ar}$  geothermometry for slowly cooled samples having a distribution of diffusion domain sizes, *J. Geophys. Res.*, *94*, 17,917-17,935, 1989.
- Lovera, O.M., F.M. Richter, and T.M. Harrison, Diffusion domains determined by Ar release during step-heating, *J. Geophys. Res.*, *96*, 2057-2069, 1991.
- Lovera, O.M., M.T. Heizler, and T.M. Harrison, Argon diffusion domains in K-feldspar II: Kinetic properties of MH-10, *Contrib. Mineral. Petrol.*, *113*, 381-393, 1993.
- Maluski, H., F. Proust, and X.C. Xiao,  $^{39}\text{Ar}/^{40}\text{Ar}$  dating of the Trans-Himalayan calc-alkaline magmatism of southern Tibet, *Nature*, *298*, 152-154, 1982.
- Mercier, J.-L., R. Armijo, P. Tapponnier, E. Carey-Gailhardis, and T.L. Han, Change from Tertiary compression to Quaternary extension in southern Tibet during the India-Asia collision, *Tectonics*, *6*, 275-304, 1987.
- Miller, D.S., I.R. Duddy, P.F. Green, A.J. Hurford and C.W. Naeser, Results of interlaboratory comparison of fission-track age standards: Fission-track workshop - 1984, *Nuclear Tracks*, *10*, 383-391, 1985.
- Molnar, P., and Tapponnier, P., 1975, Cenozoic tectonics of Asia: effects of a continental collision, *Science*, *189*, 419-426.
- Naeser, C.W., R.A. Zimmerman, and G.T. Cebular, Fission track dating of apatite and zircon: interlaboratory comparison, *Nucl. Tracks*, *5*, 65-72, 1981.
- Naeser, N.D., and H. Faul, Fission-track annealing in apatite and sphene, *J. Geophys. Res.*, *74*, 705-710, 1969.
- Pan, Y., Unroofing history and structural evolution of the southern Lhasa terrane, Tibetan plateau: implications for the continental collision between India and Asia, Ph.D. dissertation, 326 pp., State Univ. of N.Y. at Albany, 1993.
- Powell, C.M., Continental underplating model for the rise of the Tibetan plateau, *Earth Planet. Sci. Lett.*, *81*, 79-94, 1986.
- Richter, F.M., O.M. Lovera, T.M. Harrison, and P. Copeland, Tibetan tectonics from  $^{40}\text{Ar}/^{39}\text{Ar}$  analysis of a single K-feldspar sample, *Earth Planet. Sci. Lett.*, *105*, 266-278, 1991.
- Schärer, U., and C.J. Allègre, U-Pb geochronology of the Gangdese

- (Transhimalaya) plutonism in the Lhasa-Xigaze region, Tibet, *Earth Planet. Sci. Lett.*, **63**, 423-432, 1984.
- Wagner, G.A., Fission-track dating of apatites, *Earth Planet. Sci. Lett.*, **4**, 411-415, 1968.
- Xu, R.H., U. Schärer, and C.J. Allègre, Magmatism and metamorphism in the Lhasa block (Tibet): a geochronological study, *J. Geol.*, **93**, 41-57, 1985.
- Yin, A., T.M. Harrison, F.J. Ryerson, C. Wenji, W.S.F. Kidd, and P. Copeland, Tertiary structural evolution of the Gangdese Thrust System, southeastern Tibet, *J. Geophys. Res.*, **99**, 18,175-18,201, 1994.
- Zhao, W., and W.J. Morgan, Uplift of the Tibetan plateau, *Tectonics*, **4**, 359-369, 1985.
- 
- P. Copeland, Department of Geosciences, University of Houston, Houston Texas, 77204-5503 (e-mail: copeland@uh.edu)
- T.M. Harrison, Department of Earth and Space Sciences, and Institute of Geophysics and Space Physics, University of California, Los Angeles, California 90024 (e-mail: tmh@argon.ess.ucla.edu)
- W.S.F. Kidd, P. Yun, Department of Geological Sciences, State University of New York, Albany, New York 12222
- M. Royden, Department of Geology, Rensselaer Polytechnic Institute, Troy, New York 12181
- Z. Yuquan, Institute of Geochemistry, Academia Sinica, P.O. Box 91, Guyang, PRC

(Received November 29, 1993;  
revised June 17, 1994;  
accepted June 28, 1994.)